

## Supporting Information

### **Nucleobase-mediated synthesis of nitrogen-doped carbon nanozymes as efficient peroxidase mimics**

Shichao Lin,<sup>†</sup> Yihong Zhang,<sup>†</sup> Wen Cao,<sup>†</sup> Xiaoyu Wang,<sup>†</sup> Li Qin,<sup>†</sup> Min Zhou,<sup>†</sup> Hui Wei<sup>†,§,\*</sup>

<sup>†</sup>Department of Biomedical Engineering, College of Engineering and Applied Sciences, Collaborative Innovation Center of Chemistry for Life Sciences, Nanjing National Laboratory of Microstructures, Nanjing University, Nanjing, Jiangsu 210093, China.

<sup>§</sup>State Key Laboratory of Analytical Chemistry for Life Science and State Key Laboratory of Coordination Chemistry, School of Chemistry and Chemical Engineering, Nanjing University, Nanjing, Jiangsu 210093, China.

**Email:** [weihui@nju.edu.cn](mailto:weihui@nju.edu.cn); **Tel:** +86-25-83593272; **Fax:** +86-25-83594648; **Web:** [weilab.nju.edu.cn](http://weilab.nju.edu.cn)

## Table of contents

**Figure S1.** High resolution transmission electron microscopy (HRTEM) image of GNC900.

**Figure S2.** XPS spectrum of GNC900 indicating the presence of C, N, and O elements.

**Figure S3.** Thermal gravimetric analysis of GNC900 at a heating rate of 10 °C/min.

**Figure S4.** Linear calibration plot of  $A_{652}$  against glucose concentration.

**Figure S5.** Relative peroxidase-like activity of GNC900 at different storage times. Error bars represent at least three independent measurements.

**Figure S6.** Comparison of the surface area normalized peroxidase-like activities of GNC700, GNC800, and GNC900. Error bars represent at least three independent measurements.

**Table S1.** Comparison of the recent advancements and the current work in N-doped carbon nanomaterial synthesis.

**Table S2.** Contents of C, N, and O for GNC900 from XPS characterization.

**Table S3.** Contents of different N species for GNC900 from XPS characterization.

**Table S4.** Comparison of the kinetic parameters of GNC900 with other reported peroxidase mimics.  $K_m$  is the Michaelis-Menten constant,  $V_{max}$  is the maximal reaction velocity.

**Table S5.** Detection of glucose by representative carbon nanozymes based on their intrinsic peroxidase-like activity.

**Table S6.** BET surface area of nucleobase-derived carbon nanozymes.

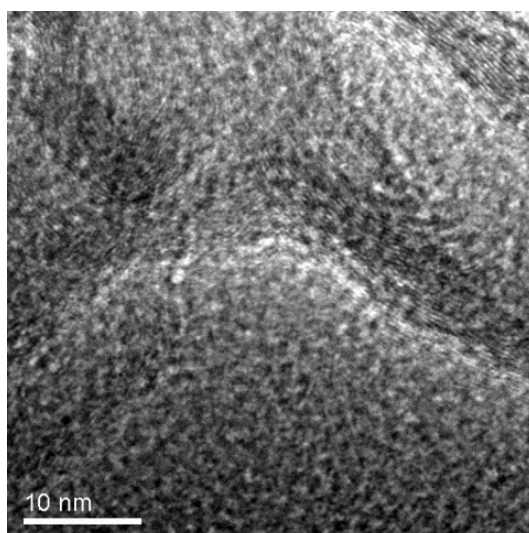


**Figure S1.** High resolution transmission electron microscopy (HRTEM) image of GNC900.

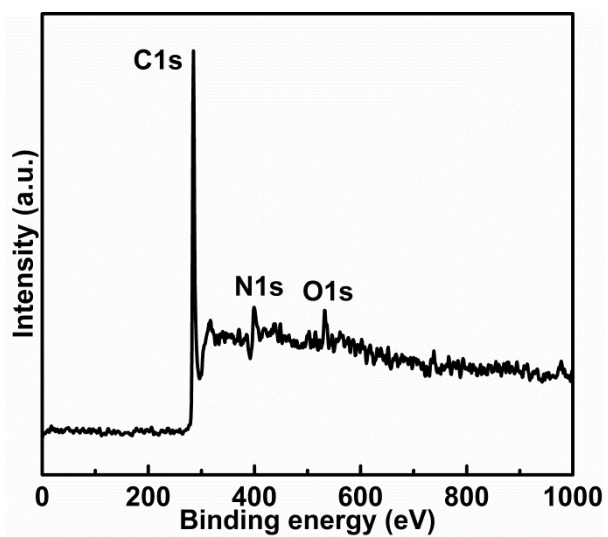


**Figure S2.** XPS spectrum of GNC900 indicating the presence of C, N, and O elements.

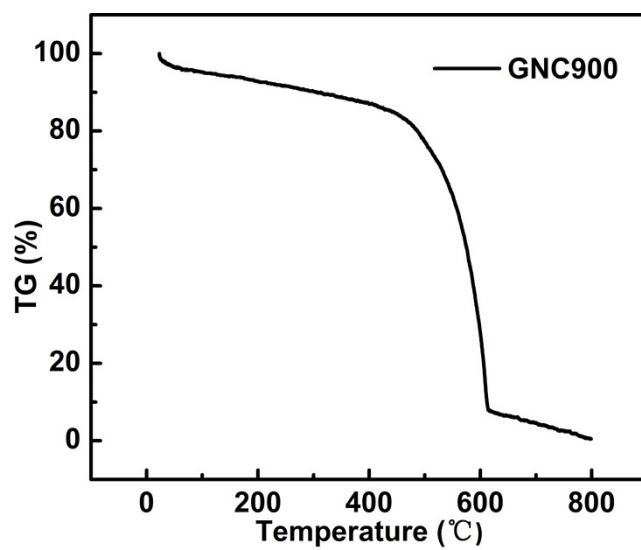


**Figure S3.** Thermal gravimetric analysis of GNC900 at a heating rate of 10 °C/min.

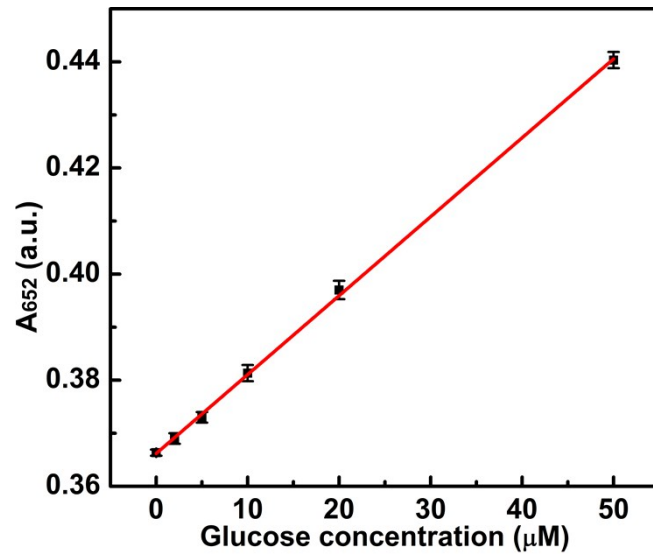


**Figure S4.** Linear calibration plot of  $A_{652}$  against glucose concentration. Error bars represent at least three independent measurements.

As shown in [Figure S4](#), it revealed a linear detection range from 2 μM to 50 μM glucose.

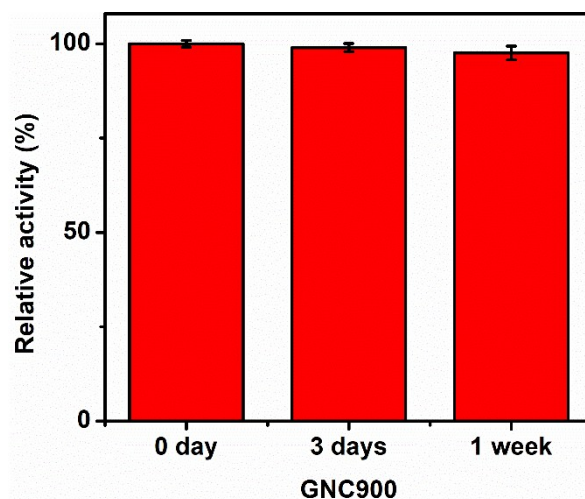


**Figure S5.** Relative peroxidase-like activity of GNC900 at different storage times. Error bars represent at least three independent measurements.

We have carried out stability test of GNC900. GNC900 dissolved in deionized water with a concentration of 0.4 mg/mL was stored for 3 days and 1 week, respectively. As shown in [Figure S5](#), GNC900 almost maintained the original peroxidase-like activity after 3 days and 1 week. This result demonstrated the high stability of our GNC900.

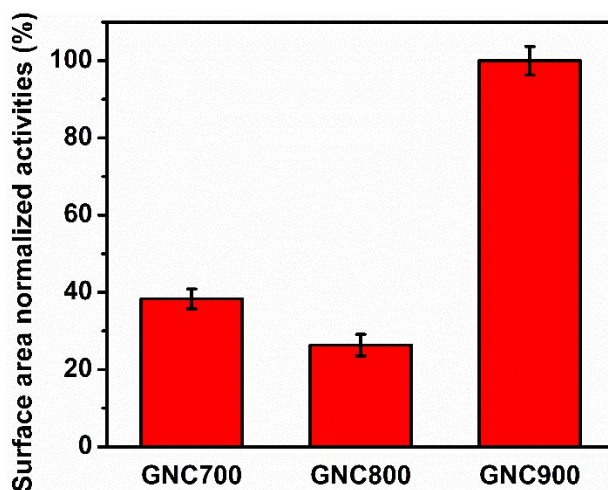


**Figure S6.** Comparison of the surface area normalized peroxidase-like activities of GNC700, GNC800, and GNC900. Error bars represent at least three independent measurements.

We have measured the surface area of GNC700, GNC800, GNC900, ANC900, CNC900, TNC900, and UNC900. Their BET surface area values are listed in [Table R1](#). It is interesting that guanine-derived N-doped carbon nanozymes exhibited higher surface areas than the ones derived from other nucleobases. Moreover, the obtained GNC maintained a high surface area under a pyrolysis temperature of 900 °C. For the surface area normalized peroxidase-like activity, GNC900 also showed the highest activity as compared to GNC800 and GNC700 ([Figure S6](#)). Together, these results demonstrated that the superior peroxidase-like activity of GNC900 was correlated with its dominant graphitic N species and its high surface area.

**Table S1.** Comparison of the recent advancements and the current work in N-doped carbon nanomaterial synthesis.

Catalyst	Multiple precursors	Template	Complex procedures	Undesired waste	Scalable production	Low cost	Reference
Nucleobases derived N-doped carbon	No	No	No	No	Yes	Yes	This work
Vertically-aligned N-doped carbon nanotube	No	No	No	Yes, NH <sub>3</sub>	No	No	<i>Science</i> , <b>2009</b> , 323, 760.
N-doped carbon hybrid microfibres	Yes	No	Yes	Yes, HNO <sub>3</sub>	Yes	No	<i>Nat. Nanotechnol.</i> <b>2014</b> , 9, 555.
N-doped carbon nanotube frameworks	Yes	No	Yes	Yes, H <sub>2</sub> SO <sub>4</sub>	No	No	<i>Nat. Energy</i> <b>2016</b> , 1, 15006.
N-doped nanoporous carbon membranes	Yes	No	Yes	Yes	No	No	<i>Nat. Commun.</i> <b>2017</b> , 8, 13592.
N-doped mesoporous carbon	Yes	Yes, SiO <sub>2</sub>	Yes	Yes	No	No	<i>J. Am. Chem. Soc.</i> <b>2017</b> , 139, 12931.
N-doped carbon dots	No	No	Yes	No	Yes	Yes	<i>Angew. Chem. Int. Ed.</i> <b>2017</b> , 56, 6459
N-doped mesoporous carbon spheres	Yes	Yes, polymer	Yes	Yes	No	No	<i>Angew. Chem. Int. Ed.</i> <b>2015</b> , 54, 588.
3D hierarchically porous N-doped carbon	Yes	Yes, cellulose ester	Yes	Yes	No	No	<i>Angew. Chem. Int. Ed.</i> <b>2014</b> , 53, 9503.
N-doped graphene	No	Yes, montmorillonite	Yes	Yes, HF	No	Yes	<i>Angew. Chem. Int. Ed.</i> <b>2013</b> , 52, 11755.
N-doped carbon nanocages	Yes	Yes, MgO	Yes	Yes, HCl	No	Yes	<i>Adv. Mater.</i> <b>2012</b> , 24, 5593.
N-doped graphene	Yes	No	Yes	Yes	No	No	<i>Chem. Mater.</i> <b>2018</b> , 30, 6431.

**Table S2.** Contents of C, N, and O for GNC900 from XPS characterization.

<b>Sample</b>	<b>C wt%</b>	<b>N wt%</b>	<b>O wt%</b>
GNC900	86.28	8.77	4.95

**Table S3.** Contents of different N species for GNC900 from XPS characterization.

Sample	Pyridinic N at%	Pyrolic N at%	Graphitic N at%	Oxidized N at%
GNC900	18.61	2.80	39.88	38.71

**Table S4.** Comparison of the kinetic parameters of GNC900 with other reported peroxidase mimics.  $K_m$  is the Michaelis-Menten constant,  $V_{max}$  is the maximal reaction velocity.

Catalyst	Substrate	$K_m$ (mM)	$V_{max}$ (Ms <sup>-1</sup> )	Ref.
GNC900	TMB	0.23	$2.53 \times 10^{-7}$	This work
GNC900	H <sub>2</sub> O <sub>2</sub>	28.3	$7.63 \times 10^{-7}$	This work
GO-COOH	TMB	0.0237	$3.45 \times 10^{-8}$	<i>Adv. Mater.</i> <b>2010</b> , 22, 2206.
GO-COOH	H <sub>2</sub> O <sub>2</sub>	3.99	$3.85 \times 10^{-8}$	<i>Adv. Mater.</i> <b>2010</b> , 22, 2206.
Pd-Ir cubes	TMB	0.13	$6.5 \times 10^{-8}$	<i>ACS Nano.</i> <b>2015</b> , 9, 9994.
Pd-Ir cubes	H <sub>2</sub> O <sub>2</sub>	340	$5.1 \times 10^{-8}$	<i>ACS Nano.</i> <b>2015</b> , 9, 9994.
Fe <sub>3</sub> O <sub>4</sub>	TMB	0.098	$3.44 \times 10^{-8}$	<i>Nat. Nanotechnol.</i> <b>2007</b> , 2, 577.
Fe <sub>3</sub> O <sub>4</sub>	H <sub>2</sub> O <sub>2</sub>	154	$9.78 \times 10^{-8}$	<i>Nat. Nanotechnol.</i> <b>2007</b> , 2, 577.
HRP	TMB	0.434	$10 \times 10^{-8}$	<i>Nat. Nanotechnol.</i> <b>2007</b> , 2, 577.
HRP	H <sub>2</sub> O <sub>2</sub>	3.7	$8.71 \times 10^{-8}$	<i>Nat. Nanotechnol.</i> <b>2007</b> , 2, 577.

**Table S5.** Detection of glucose by representative carbon nanozymes based on their intrinsic peroxidase-like activity.

Peroxidase mimics	Catalyst concentration	Detection time	Linear range	Limit of detection	Reference
GNC900	10 µg/mL	30 min + 20 min	2.5-50 µM	1.14 µM	This work
GO-COOH	40 µg/mL	1 h + 10 min	1-20 µM	1 µM	<i>Adv. Mater.</i> <b>2010</b> , <i>22</i> , 2206.
C-Dots	1 µg/mL	30 min + 30 min	1-500 µM	0.4 µM	<i>Chem. Commun.</i> <b>2011</b> , <i>47</i> , 6695.
C <sub>60</sub> [C(COOH) <sub>2</sub> ] <sub>2</sub>	20 µM	30 min + 2 h	1-40 µM	0.5 µM	<i>Biosens. Bioelectron.</i> <b>2013</b> , <i>47</i> , 502
SWCNH-COOH	25 µg/mL	30 min + 15 min	100-2000 µM	100 µM	<i>Analyst</i> , <b>2015</b> , <i>140</i> , 6398.

**Table S6.** BET surface area of nucleobase-derived carbon nanozymes.

Nanozymes	BET surface area (m <sup>2</sup> /g)
GNC700	358.0883
GNC800	659.6481
GNC900	493.7293
ANC900	8.5763
CNC900	16.9208
TNC900	54.2764
UNC900	10.5649